DOI: 10.1002/cphc.200700357

The Molecular Orientation of para-Sexiphenyl on Cu(110) and Cu(110) p(2×1)O

Martin Oehzelt,*[a] Leonhard Grill,[b] Stephen Berkebile,[a] Georg Koller,[a] Falko P. Netzer,[a] and Michael G. Ramsey[a]

Controlling the molecular growth of organic semiconductors is an important issue to optimize the performance of organic devices. Conjugated molecules, used as building blocks, have an anisotropic shape and also anisotropic physical properties like charge transport or luminescence. The main challenge is to grow highly crystalline layers with molecules of defined orientation. The higher the crystallinity, the closer these properties reach their full intrinsic potential, while the orientation determines the physical properties of the film. Herein we show that the molecular orientation and growth can be steered by the surface chemistry, which tunes the molecule–substrate interaction. In addition, the oxygen reconstruction of the surface, demonstrates the flexibility of the organic molecules to adopt a given surface corrugation and their unique possibility to release stress by tilting.

Introduction

The growth of molecules on inorganic substrates, especially for semiconducting organic materials, has attracted both scientific and technological interest in recent years.[1,2] The understanding and tailoring of the initial growth of ordered thin films is one key challenge that needs to be tackled for organic devices in order to exploit their full technological potential.[3] Small aromatic molecules like *para*-sexiphenyl (6P: $C_{36}H_{24}$), technologically relevant and used, for example, in blue light-emitting diodes,[4] are good model materials for growth studies. One way to achieve ordered growth is to deposit molecules onto an ordered substrate that serves as a template. In particular, anisotropic substrates with a large surface corrugation are attractive as they have the ability to orient the molecules uniaxially.[5–7] Up to now, studies were carried out for given molecule–substrate combinations where the growth was steered by controlling the substrate temperature and the growth rate. However, this parameter space is very limited and enhanced control on the crystal-growth mode is desired. In this paper, we show that the role of the substrate is not solely to serve as a solid support for the growing thin film, but can also determine the interaction between the molecules and thus the growth character in a specific orientation. This change results in very different adsorption geometries of the monolayers with direct influence on further film growth.

Recent studies on 6P have shown that a graphitic carbon layer on gold strongly influences the organic growth.[8] On clean gold the first organic layer consists of flat lying molecules and lying molecules which have their molecular planes tilted by 66° with respect to the substrate.[9] In contrast, on the carbon precovered substrate the molecular plane tilt is constant in the monolayer, but their relative in-plane orientation is randomly distributed due to the lack of order in the graphitic layer. An other approach is to deposit molecules with functional groups (i.e. NDCA,[10] trimellatic acid,[11] and many more) on ordered substrates. There, the enhanced interaction between the molecules and/or to the substrate compared to the pure hydrocarbon systems can be used to control the organic growth. In contrast to these studies we have concentrated on a pure hydrocarbon material (6P) and have deposited the molecules on a single crystalline substrate as well as on an ordered surface reconstruction.

The Cu(110) surface, used as substrate, has a surface structure of tightly packed copper rows that are oriented along the [1-10] direction. It provides an unidirectional corrugation and rod-like molecules are expected to orient along this direction.[5,12] The Cu(110) p(2×1)–O surface reconstruction has an even more pronounced corrugation with close-packed Cu–O rows oriented along [001]. Moreover, the chemistry of the surface is also changed because Cu–O is a less reactive surface than pure copper. Dosing less oxygen generates the so-called striped phase, where alternating stripes of copper and copper–oxygen are formed in an ordered array.[13]

[a] *Dr. M. Oehzelt,[+] S. Berkebile, Dr. G. Koller, Prof. Dr. F. P. Netzer, Prof. Dr. M. G. Ramsey*
Institute of Physics, Surface and Interface Physics
Karl-Franzens Universität Graz
Universitätsplatz 5, 8010 Graz (Austria)
Fax: (+43) 316-380-9816
E-mail: martin.oehzelt@jku.at

[b] *Dr. L. Grill*
Institut für Experimentalphysik, Freie Universität Berlin
Arnimallee 14, 14195 Berlin (Germany)

[+] *Current address: Institut für Experimentalphysik*
Abteilung für Atom- und Oberflächenphysik
Johannes Kepler Universität Linz
Altenbergerstraße 69, 4040 Linz (Austria)
Fax: (+43) 732-2468-8509

Results and Discussion

Figure 1 summarizes the evolution of the valence band structure for the growth of 6P films on Cu(110), Cu(110) p(2×1)–O, and Cu(110)–O striped, at room temperature. On all three surfaces the work function decreases steeply upon molecular adsorption until the change saturates when the surface is covered by a molecular monolayer.[14] For the clean Cu and the fully reconstructed (2×1)–O substrates the monolayers are completed after ≈3 Å and ≈6 Å 6P deposition, respectively. For the striped phase (50% covered with Cu(110)–O) it is at an intermediate value of ≈4.5 Å. The most significant differences in the photoemission spectra of the monolayer covered substrates are in the region of the Fermi energy (E_F), where no orbitals of the pristine molecule exist. On copper (Figure 1a) significant emission is seen at E_F that decreases in intensity at coverages above the monolayer (3 Å). This is clearly indicative of a backdonation bond of 6P with Cu electrons of the substrate which are transferred to the molecular π-states partially filling the LUMO.[15] In contrast, on Cu(2×1)–O (Figure 1c) the valence band spectra show no evidence for such a charge transfer as no enhanced emission at E_F (compared to the pristine substrate) is detected. Comparing the monolayer spectra of these two cases in Figures 1a and c, one sees that the orbital emissions in the region of −6 eV binding energy are very weak on Cu but clearly visible on the Cu–O substrate. This suggests a different molecular adsorption geometry on the two substrates, because photoemission intensities are determined by selection rules, which are in turn determined by the adsorption geometry. Thus, different geometries on the two surfaces can be concluded.

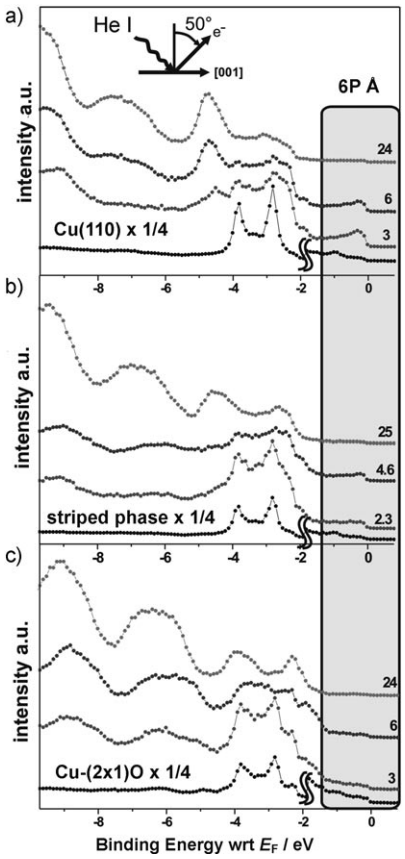

Figure 1. Thickness-dependent ARUPS signal of 6P on a) Cu(110), b) on the partly and c) on the fully reconstructed (2×1)O surface. Spectra of different thicknesses are shifted for clarity. The marked region highlights the enhanced density of states at the Fermi level for very thin films. Due to their intense d-band features, the substrate spectra have been reduced by a factor of four below 2 eV binding energy. The experimental geometry is shown in the inset and is the same for all shown spectra.

Low temperature scanning tunnelling microscopy (LT-STM) images from low coverages of 6P on clean copper, on the Cu–O striped phase and on the Cu(2×1)–O surface are depicted in Figures 2a, b and c, respectively. It turns out that the orientation of 6P is different on the three substrates; on pure copper the orientation is predominantly along [1-10], while on the copper regions of the striped phase and on the fully covered Cu(2×1)O surface it is along [001] (forming a (2×15) commensurate overlayer with respect to the clean Cu(110) surface). The most outstanding difference regards the packing density. For submonolayer exposures on the Cu(2×1)–O, the molecules form densely packed islands, while on the pure copper surface they do not form islands but are dispersed over the entire surface. These differences are consistent with the photoemission spectra where the monolayer density is inferred from the workfunction saturation.[14] The rather large distances between the molecules on the copper terraces can be explained in terms of repulsive intermolecular interactions, which is in strong contrast to the aggregation into islands on Cu(2×1)–O as a result of intermolecular attraction. At the highest density of the molecules on copper, the closest lateral intermolecular spacing observed is 10.2 Å (see for instance Figure 2b), almost twice that between 6P molecules in a bulk crystal. The backdonation observed in the ARUPS spectra is presumably the origin

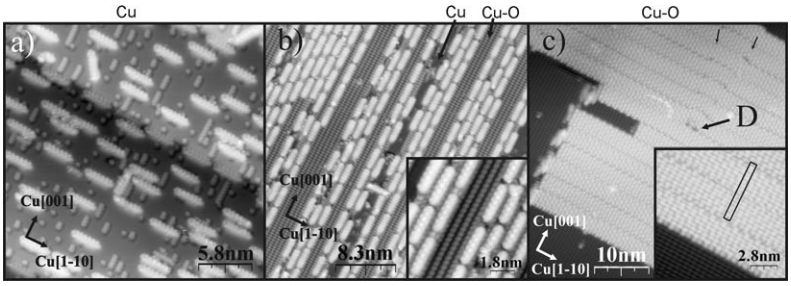

Figure 2. STM images of 6P deposited on a) Cu(110), b) the partly and c) the fully oxygen reconstructed (2×1)–O surface. In all three cases a CO molecule was adsorbed on the STM tip apex for enhanced contrast. The copper surface directions are indicated and the insets show images with higher resolution. The small arrows at the top of the image in (c) indicate dislocations in the overlayer. The inset of (c) shows the unit cell (5.1 Å×54.1 Å). Tunneling current I = 0.1 nA and bias voltage U = +1.0 V for all images except for the inset of (b) with U = −0.5 V.

of the repulsion. The mechanism behind the repulsion could either be direct electrostatics due to a charge transfer from the substrate to the molecules or surface mediated as the backdonation is typically concomitant to a simultaneous donation.

On the fully reconstructed (2×1)–O surface, for very low exposures, the molecules adsorb at defects, which act as nucleation centers for island growth. Initially, these islands appear as single columns of molecules stacked side-by-side with their molecular axes parallel to the Cu–O rows (i.e. [001]) and are elongated along [1-10] (see Figure 3). With further deposition large, highly ordered two-dimensional islands are formed by aggregation of the columns (Figure 2c). On the (2×1)–O substrate each molecule appears to have seven or eight maxima separated by 3.6 Å, which is the periodicity of the substrate. As a CO molecule has been attached to the STM tip before imaging (to enhance the contrast), an exact interpretation is not straightforward, but the result suggests that the image reflects not only the molecules themselves, but also the modification of the tunneling probability to the copper atoms in the added row structure.

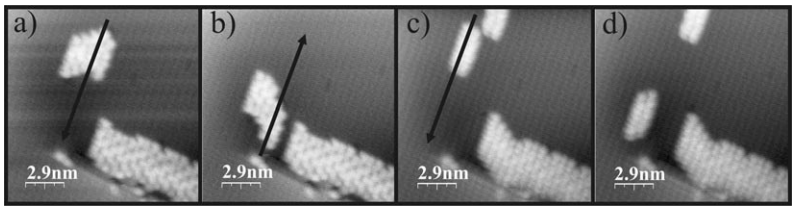

Figure 3. Molecular manipulation in [001] direction. A series of STM images of successive molecular manipulations on a single column of molecules on the (2×1)–O surface is shown in a)–d). Arrows indicate the tip pathway during the subsequent manipulation. Bias voltage $U=+1.0$ V and tunneling current $I=5$ pA for all images. Tunneling resistance during lateral manipulation between 10^8 and 10^9 Ω.

Molecular manipulation along [001] (Figure 3) illustrates the intermolecular interactions on the Cu(2×1)–O surface. The initial group of five molecules has been removed from the molecular column. In subsequent manipulations (Figure 3b–d), the relative position between the molecules in [001] direction is changed, but their spacing in the [1-10] direction remains the same. Thus, the (2×1)–O corrugation acts as rails, maintaining the molecular orientation during manipulation. This coordinated movement shows that the interaction between neighboring molecules is attractive and strong. An attractive intermolecular interaction rules out an adsorption geometry with the aromatic planes parallel to the surface (also inferred by the small intermolecular distances). Only with the molecular planes tilted with respect to the surface, a significant van der Waals interaction between the π-orbitals can occur. Each manipulation offsets the molecules and finally causes island scission. Even after multiple displacements the smallest entity that could be imaged was a dimer. In contrast to the movement along [001], it was impossible to move the molecules in the perpendicular direction, that is, across the substrate rows, even for very large forces at small tip-substrate distances.[16]

STM images taken with a particular modified tip (Figure 4) show an alternating contrast and different molecular appearance in neighboring columns of an island. We believe that this reflects an alternating molecular tilt angle within a 6P (20−3) plane of the bulk crystal structure[17] (inset of Figure 4). X-ray diffraction measurements from thicker films (30 nm, which corresponds to about 80 lying molecular layers, Figure 5) grown on this substrate reveal that the 6P(20-3) planes are indeed parallel to the substrate with all molecules uniaxially oriented along the [001] direction (see Figure 4).[18] The (20−3) bulk plane has a two dimensional unit cell with dimensions of 5.565 Å×54.603 Å and the 6P is organized in columns of molecules with the long molecular axis perpendicular to the columns but parallel to the substrate surface rows.[17] Within the columns of the (20-3) plane all molecules have their molecular plane tilted by 33° alternating from column to column (see insert in Figure 4). Comparing the bulk crystal plane with the observed surface layer shows a compression of −8.4% in the [1-10] direction and of −1.1% in the [001] direction. Given the rather weak substrate–molecule interaction, it seems unlikely that the observed surface layer is simply a compressed (20-3) bulk plane forced by the substrate. High pressure XRD meas-

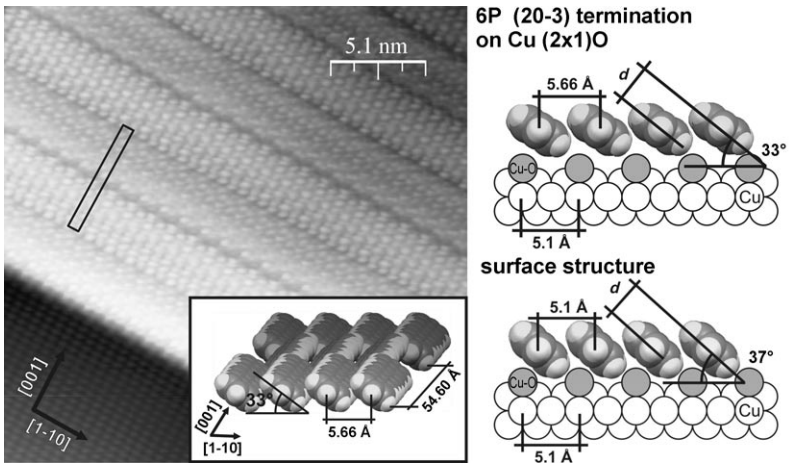

Figure 4. The STM image shows an island of 6P on the fully reconstructed (2×1)–O surface. The different contrast of neighbouring columns results presumably from a molecular fragment, not CO (see Figure 2c), at the tip apex. The inset shows a model of the 6P(20−3) plane of the bulk crystal structure. The models on the right illustrate the proposed stress release model. (bias voltage $U=+1.0$ V and tunneling current $I=1.0$ nA)

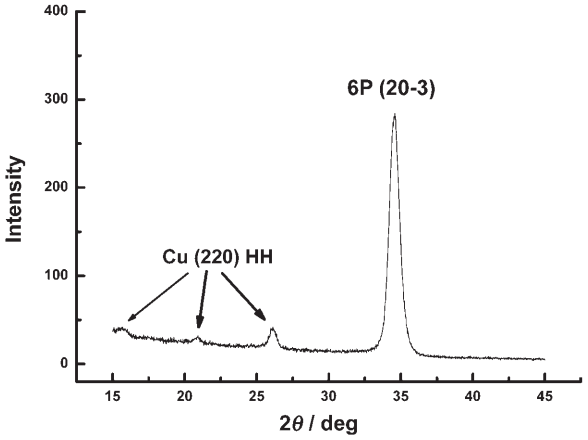

Figure 5. Specular $\theta/2\theta$ scan of the thick 6P film on Cu(110)–(2×1)O. The major peak at $2\theta = 34.5^\circ$ originates from the (20-3) oriented 6P. The small peaks at lower angles are higher harmonics of the copper substrate.

urements have shown that pressures of one to two GPa[18] would be required to compress the lattice of 6P by this amount. This is well beyond stresses known from thin-film growth of inorganic materials which are typical in the MPa region. Instead, we propose that, by altering the inclination of the individual molecular planes with respect to the surface, the molecules can decrease their distance to each other without applying significant forces and keeping the distances between their molecular planes constant, as illustrated in Figure 4. A simple model to estimate the change of the tilt angle (keeping the van der Waals distances—of the bulk crystal structure—constant and increasing the tilt angle until the intermolecular distance reaches the observed value of 5.1 Å) shows that a rotation of the molecular planes by only 4° is sufficient to allow commensurability without compromising the van der Waals spacing. This is a new stress release mechanism only made possible due to the anisotropy of the building blocks within the film.

In order to confirm this hypothesis, we have performed polarisation dependent C 1s–NEXAFS (near-edge x-ray absorption fine structure spectroscopy) measurements. If the molecules have the ability to release stress by increasing their tilt angle at the interface, a different inclination angle in the monolayer and the 6P(20-3) crystallites, growing on it, should be seen in the C 1s→π* resonance. For normal incidence with the polarization plane parallel to [001], the π* excitation should be forbidden for both the monolayer and the multilayer films if the molecular axes are parallel to the surface and the [001] azimuthal direction. This is indeed observed, in perfect agreement with the orientation derived above. In [1-10] direction, perpendicular to the molecules, the inclination angle of the molecules with respect to the substrate can be determined from the π* intensity variations.[19,20] NEXAFS spectra of the monolayer (Figure 6a) exhibit a strong C 1s→π* resonance that does not change upon a variation of the photon incidence angle θ as can be seen in the inset. In contrast, the intensity of the C 1s→π* resonance for the thick layer (≈32 nm) changes considerably upon increasing the incidence angle θ (inset of Figure 6b).

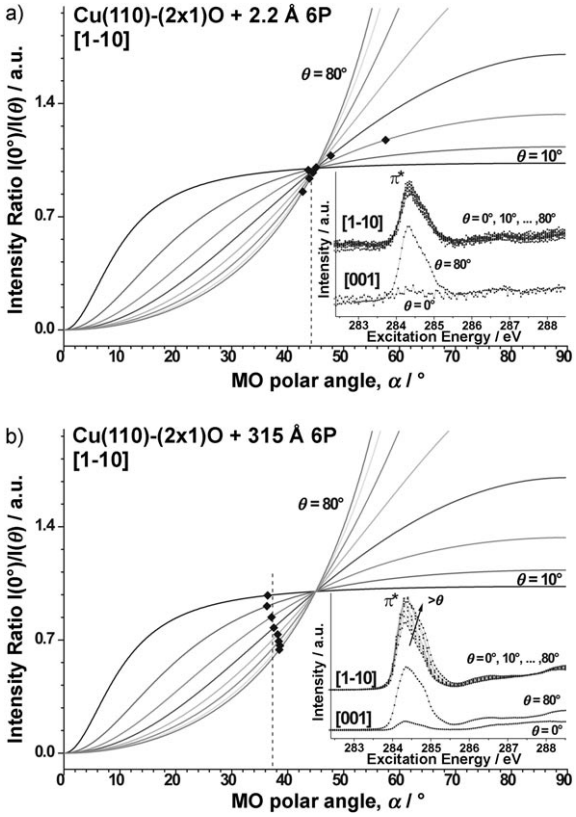

Figure 6. NEXAFS spectra of 6P on the fully reconstructed (2×1)–O surface. Calculated intensity ratio plots $I(\theta=0^\circ)/I(\theta)$ as a function of the π*-orbital (MO) tilt angle (α) for various X-ray incidence angles (taking the two-fold symmetry of the substrate into account), together with experimentally determined C 1s→π* transition ratios (solid symbols) for a) 6P monolayer, b) 315 Å thick 6P(20-3) film. The dashed vertical lines indicate the derived molecular tilt angles with respect to the substrate. The respective NEXAFS spectra are shown in the insets.

To determine the molecular tilt angle, the calculated intensity ratio plots $I(\theta=0^\circ)/I(\theta)$ are shown as a function of the π*-orbital vector tilt angle α and for various X-ray incidence angles θ, together with the experimentally determined C 1s→π* transition ratios. The resulting tilt angle of the molecular plane in the case of the monolayer on the (2×1)–O reconstructed surface is determined to be $44^\circ \pm 5^\circ$ (Figure 6a). The same experiment for the thick film (b) reveals an angle of $37^\circ \pm 5^\circ$. Although there is a systematic error making the results of both systems slightly larger than expected, the decrease in tilt angle from the monolayer to the thick bulk-like film is significant and reproducible and fully supports the proposed geometrical model.

Exposing the Cu(110) surface to less oxygen than in the fully reconstructed case leads to the striped phase, with regions of Cu–O rows separated by regions of bare copper.[13] An example of 6P deposited on the striped Cu–O surface is given in Figure 2b. It seems that the 6P molecules initially adsorb on the Cu stripes at the boundary to the Cu–O rows and then cover the clean Cu regions, in accordance to the stronger interaction with Cu. The presence of the Cu–O rows leads to a reorientation of the molecules adsorbed on the clean Cu regions from parallel to the Cu rows, to perpendicular to them (i.e. parallel

to the O rows). 6P is mainly organized in strings of molecules with typical distances between molecules of 28.8 Å, 30.6 Å and 32.4 Å, which corresponds to 8, 8.5 or 9 times the distance of close-packed copper rows in [001] direction, respectively, thus following the periodicity of the substrate. In addition, the relative position of molecules in neighboring rows is rather stochastic than predefined. The separation between the molecular rows in [1-10] direction is 10.2 Å and equals four times the periodicity of the copper substrate in this direction. This growth is reminiscent of the growth on the clean copper surface but with the exception of the orientation of the molecules; on the latter, they are oriented along [1-10].

The registry of the 6P molecules on clean copper and those reoriented by the presence of Cu–O is determined in Figure 7.

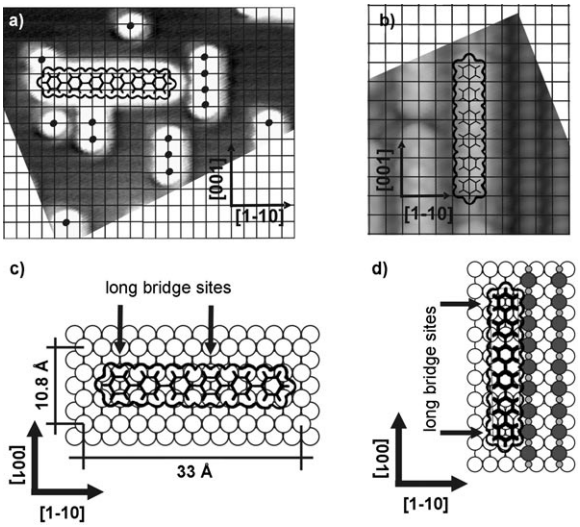

Figure 7. 6P registry on the Cu(110) and on the striped Cu–O surface. a) One 6P molecule on copper with CO seen as white blobs in its vicinity. The centre of the CO is marked by a black dot, which determines the position of the copper surface atoms. b) One 6P molecule on the striped Cu–O surface. The regular protrusions on the right hand side of the image originate from copper atoms of the (2×1)–O stripes, which were used to draw the net of copper surface atoms. The models to the STM images are shown in c) for copper and d) for the striped Cu-O surface. Bias voltages $U=-1.0$ V (a), and $U=-0.5$ V (b). Tunnelling current $I=0.1$ nA for (a) and (b).

In contrast to previous studies,[21] it is not necessary to build artificial structures of adatoms in the vicinity of the molecules to determine their registry. In Figure 7a the adventitious CO molecules serve as markers for on-top sites[22] while in Figure 7b the neighboring (2×1)–O lattice allows the copper surface mesh to be defined.[23] The resulting meshes in Figure 7a and b represent the underlying copper lattice. For clean copper the adsorption site of the molecule is shown in Figure 7c with both the structure of the molecule and its van der Waals size. The molecules are adsorbed in the troughs between the close-packed copper rows along [1-10] such that two phenyl rings occupy long bridge sites. Both the 1, 4 (as illustrated) and 2, 5 rings in long-bridge positions are observed for various molecules on the clean copper surface. When the molecules are reoriented across the copper corrugation the determining factor again appears to be the maximization of the number of the long-bridge sites (see Figure 7d). Significantly, the molecules align across the top of the copper atoms rather than across the short-bridge sites of the copper rows, where one might intuitively expect it, to allow long-bridge sites. Previous studies on Ni(110) have shown that 6P tends to maximize the preferred adsorption sites of the phenyl rings.[24] In the case of Ni(110), the preferred adsorption site of the benzene monomer is the hollow site and the resulting adsorption sites of 6P are different to those observed here on Cu(110). For benzene on Cu(110), both experiments[25] and theoretical calculations[26,27] have revealed that the long-bridge sites are preferred. In the case of 6P on the less reactive (2×1)–O surface, where the aromatic planes are tilted, the determination of the exact registry is more difficult, even though the periodicity is clear in the STM images. Although there is nearly perfect commensurability in [1-10], due to the strong corrugation in this direction, the position along the rows is not as well specified. An illustration of this is seen in the dislocations (marked by two small arrows in the upper right corner) radiating from a point defect (D) in Figure 2c, where the molecules are displaced along the [001] direction. Clearly, the weaker bond to the substrate leads to a less preferred adsorbate registry.

Conclusions

We conclude that a weak interaction to the substrate and therefore a growth dominated by attractive intermolecular interactions is desirable to form highly ordered organic interfacial layers. In contrast, strong molecule-substrate interactions disturb the molecules' ability to self-assemble. Therefore highly ordered organic interface structures, needed for optimal crystalline thin films, require substrate surfaces that give the molecules a direction without strongly perturbing their ability to organize into a near bulk crystal plane. Small deviations from the bulk crystal structure can be adopted by the molecules to a certain extend due to their unique property to release stress by tilting.

The registry of the molecules on the copper surface and on the copper regions of the (2×1)O suggests that the *para*-sexiphenyl molecule tries to maximize the number of preferred adsorption sites of its phenyl rings. This tendency could lead to a general rule for the determination of adsorption sites of bigger molecules through their subunits, but to prove this theory many other molecule–substrate combinations have to be studied.

Experimental Section

All experiments are performed in ultra high vacuum (UHV) with pressures in the region of low 10^{-10} mbar or better. The UV-photoemission results were obtained at the KFU Graz and the low-temperature scanning tunneling microscopy measurements were done at the FU Berlin, the instruments are described elsewhere.[28,29] The near edge X-ray absorption fine structure (NEXAFS) measurements were performed using the Mustang end-station at the RG-BL of BESSY II. The NEXAFS measurements were performed with photon angles of incidence from normal ($\theta=0°$) to grazing ($\theta=80°$) along the high symmetry directions [001] and [1-10]. All chambers have

basic surface cleaning facilities which are used to clean the substrates with repeated cycles of ion sputtering and annealing at 800 K. Dosing 10 L [1 Langmuir (L) = 1×10^{-6} Torr sec] of oxygen on the clean Cu(110) crystal forms a p(2×1) added row reconstruction which chemically polishes the surface. The resulting terraces are up to hundreds of nanometers wide and separated by monoatomic steps. In addition, oxygen exposure not only flattens out the substrate but also passivates it. The striped phase is prepared by exposing the clean copper surface to 1.5 L oxygen which generates a periodic structure of alternating regions of clean Cu and Cu–O regions.[13]

6P molecules (Tokyo Chemical Industry Co. Ltd.) were evaporated from a molecule evaporator, which allowed film growth at residual pressures below 5×10^{-10} mbar. The substrate was held at room temperature during deposition and nominal growth rates of 1 Å min^{-1} were used, as monitored with a quartz microbalance. Note that the monolayer for clean copper and Cu–O have thicknesses of ≈3 Å and ≈6 Å, respectively, due to the different packing of the molecules in the first monolayer.

After deposition (at room temperature), the sample was cooled to liquid helium temperature and transferred to the STM. The LT-STM system was operated at a temperature of about 7 K. An electrochemically etched tungsten wire was used as STM tip for the present experiments. Prior to the measurements the final tip condition was optimized by controlled tip-sample contact at 7 K and therefore the tip apex is presumably covered by copper atoms. Different contrasts in the STM images are due to different adsorbates on the tip apex. For instance, CO was intentionally picked up by STM manipulation and subsequently recorded images (Figure 2 and Figures 3c–d) show an enhanced contrast. In Figure 4 presumably a 6P molecule or a molecular fragment was adsorbed on the tip apex. All tunneling voltages indicated in the figures refer to the sample bias with respect to the tip.

The X-ray diffraction $\theta/2\theta$ measurements were carried out ex-situ with a PHILIPS X'PERT system with $Cr_{K\alpha}$ radiation. On the detector side a flat graphite monochromator was used.

Acknowledgements

This work was supported by the Austrian Science Fund (FWF) and by the European Integrated Project PICO INSIDE. We also like to acknowledge the assistance of G.-N. Gavrila with the MUSTANG end-station at RG-BL of BESSY II and R. Resel for the XRD measurements (Figure 5).

Keywords: crystal growth · hydrocarbons · self-assembly · surface chemistry · stress release

[1] J. R. Sheats, H. Antoniadis, M. Hueschen, W. Leonard, J. Miller, R. Moon, D. Roitman, A. Stocking, *Science* **1996**, *273*, 884–888.
[2] G. Witte, C. Wöll, *J. Mater. Res.* **2004**, *19*, 1889–1916.
[3] F. Yang, M. Shtein, S. R. Forrest, *Nat. Mater.* **2005**, *4*, 37–41.
[4] G. Leising, S. Tasch, F. Maghdadi, L. Athouel, G. Froyer, U. Scherf, *Syn. Met.* **1996**, *81*, 185–189.
[5] M. Oehzelt, G. Koller, J. Ivanco, S. Berkebile, T. Haber, R. Resel, F. P. Netzer, M. G. Ramsey, *Adv. Mater.* **2006**, *18*, 2466–2470.
[6] G. Koller, S. Berkebile, J. R. Krenn, F. P. Netzer, M. Oehzelt, T. Haber, R. Resel, M. G. Ramsey, *Nano Lett.* **2006**, *6*, 1207–1212.
[7] S. Berkebile, G. Koller, G. Hlawacek, C. Teichert, F. P. Netzer, M. G. Ramsey, *Surf. Sci.* **2006**, *600*, L313–L317.
[8] S. Müllegger, A. Winkler, *Surf. Sci.* **2006**, *600*, 1290–1299.
[9] S. Müllegger, K. Hänel, T. Strunskus, C. Wöll, A. Winkler, *ChemPhysChem* **2006**, *7*, 2552–2558.
[10] J. Taborski, V. Wüstenhaben, P. Väterlein, E. Umbach, *Chem. Phys. Lett.* **1995**, *239*, 380–386.
[11] A. Dmitriev, H. Spillmann, S. Stepanow, T. Strunskus, C. Wöll, A. P. Seitsonen, M. Lingenfelder, N. Lin, J. V. Barth, K. Kern, *ChemPhysChem* **2006**, *7*, 2197–2204.
[12] Y. Hu, K. Maschek, L. D. Sun, M. Hohage, P. Zeppenfeld, *Surf. Sci.* **2006**, *600*, 762–769.
[13] K. Kern, H. Niehus, A. Schatz, P. Zeppenfeld, J. Goerge, G. Comsa, *Phys. Rev. Lett.* **1991**, *67*, 855–858.
[14] G. Koller, B. Winter, M. Oehzelt, J. Ivanco, F. P. Netzer, M. G. Ramsey, *Org. Electron.* **2007**, *8*, 63–68.
[15] F. P. Netzer, M. G. Ramsey, *Crit. Rev. Solid State Mater. Sci.* **1992**, *17*, 397–475.
[16] L. Grill, F. Moresco, P. Jiang, C. Joachim, A. Gourdon, H.-K. Rieder, *Phys. Rev. B* **2004**, *69*, 035416 1–7.
[17] K. N. Baker, A. V. Fratini, T. Resch, H. C. Knachel, W. W. Adams, E. P. Socci, B. L. Farmer, *Polymer* **1993**, *34*, 1571–1587.
[18] G. Heimel, P. Puschnig, M. Oehzelt, K. Hummer, B. Koppelhuber-Bitschnau, F. Porsch, C. Ambrosch-Draxl, R. Resel, *J. Phys. Condens. Matter* **2003**, *15*, 3375–3389.
[19] J. Stöhr, D. A. Outka, *Phys. Rev. B* **1987**, *36*, 7891–7905.
[20] J. Stöhr, *NEXAFS Spectroscopy, Springer Series in Surface Science* (Eds: G. Ertle, R. Gomer, D. L. Mills), Springer, Heidelberg, **1992**.
[21] J. Lagoute, K. Kanisawa, S. Fölsch, *Phys. Rev. B* **2004**, *70*, 245415 1–6.
[22] Ph. Hofmann, H.-M. Schindler, S. Bao, V. Fritzsche, A. M. Bradshaw, D. P. Woodruff, *Surf. Sci.* **1995**, *337*, 169–176.
[23] C. Corriol, J. Hager, R. Matzdorf, A. Arnau, *Surf. Sci.* **2006**, *600*, 4310–4314.
[24] G. Koller, S. Surnev, M. G. Ramsey, F. P. Netzer, *Surf. Sci.* **2004**, *559*, L187–L193.
[25] M. Doering, H.-P. Rust, B. G. Briner, A. M. Bradshaw, *Surf. Sci.* **1998**, *410*, L736–L740.
[26] R. L. Rogers, J. G. Shapter, M. J. Ford, *Surf. Sci.* **2004**, *548*, 29–40.
[27] A. Bilic, J. R. Reimers, N. S. Hush, R. C. Hoft, M. J. Ford, *J. Chem. Theory Comput.* **2006**, *2*, 1093–1105.
[28] G. Koller, R. I. R. Blyth, S. A. Sardar, F. P. Netzer, M. G. Ramsey, *Surf. Sci.* **2003**, *536*, 155–165.
[29] G. Meyer, *Rev. Sci. Instrum.* **1996**, *67*, 2960–2965.

Received: May 21, 2007
Published online on June 22, 2007

